pH-Controlled Assemblies of Polymeric Amine-Stabilized Gold Nanoparticles

Rajesh Sardar, Natalie S. Bjorge, and Jennifer S. Shumaker-Parry*

Department of Chemistry, University of Utah, 315 South 1400 East, RM 2020, Salt Lake City, Utah 84112

Received February 22, 2008; Revised Manuscript Received April 10, 2008

ABSTRACT: The pH-controlled assembly of gold nanoparticles within a polymer−gold nanoparticle (AuNP) composite material is described. Poly(allylamine) (PAAm) is used as a reducing and stabilizing agent to generate a stable water-soluble polymer−AuNPs composite. The optical properties and the morphology of the composite material are sensitive to the solution pH due to structural changes of the polymer. As a result, the nanoparticles undergo reversible assembly/dispersion processes controlled by the solution pH. The role of the PAAm in the formation of the assemblies is confirmed by infrared spectroscopy and place exchange reactions.

Introduction

Applications of metal nanoparticles in optical and electronic detection systems,[1–3] medical diagnostics,[4] surface-enhanced Raman scattering (SERS),[5–7] and the development of optical devices[8–10] have inspired much nanotechnology research activity. In this context, polymer-stabilized metal nanoparticle composites are of special interest because polymers can be used to tailor the properties of nanoparticle assemblies.[11–19] In addition, incorporation of nanoparticles into the polymer matrix can modify the physical properties of the polymer.[20,21] The combination of the properties of nanoparticles (e.g., optical) and macromolecules (e.g., swelling or shrinking) provides an avenue to prepare composite materials with unique properties compared to the individual nanoparticle and polymer components. In this respect, polymer−nanoparticle composite materials have been used in storage media,[22] catalysis,[23–26] and sensor development.[27]

A challenge in tailoring polymer−nanoparticle composite materials for applications is the control of the organization of nanoparticles inside the polymer matrix. The nanocomposite properties are strongly related to the dispersion of particles inside the polymer matrix as well as the polymer structure.[28,29] Literature reports showed that the attraction between nanoparticles and polymer is essential in order to disperse the particles and control the organization for specific applications.[30,31] Control of pH could be one approach for tailoring the polymer structure and ultimately the organization of nanoparticles in the composite. For example, when the polymer contains basic or acidic groups, the degree of protonation or deprotonation can be used to control electrostatic interactions which influence the organization of the polymer structures and ultimately the dispersion of the nanoparticles within the polymer.

In most studies to date, the effects of pH on the organization of polymer−gold nanoparticles (AuNPs) composite materials have been investigated using AuNPs (diameter >10 nm) which were further functionalized after synthesis with different synthetic polymers or biopolymers.[27,32–34] In all of these systems the polymers contained functional groups that could be cycled between protonation or deprotonation as the pH was changed. In most cases, the nanoparticle surface was functionalized with polymers containing an amine terminal group, and dispersion of AuNPs in the solution or sample matrix was induced at an acidic pH due to electrostatic interactions. The surface plasmon resonance (SPR) properties of the nanoparticle assemblies in the composites also have been investigated. A shift in the SPR band was observed upon variation of solution pH for AuNPs functionalized with poly(4-vinylpyridine). This shift was likely due to the dispersion or formation of an aggregated state as the charge on the polymer changed.[33]

In a recent report we described a simple route of gold nanoparticle (diameter <3 nm) synthesis using poly(allylamine), PAAm, as both reducing and stabilizing agent to form a PAAm−AuNPs composite.[35] The dual role of the polymer in the synthetic method eliminates the need for an additional surfactant which could alter the nanocomposite properties as well as restrict its application. In addition, the advantage of preparing a composite composed of small particles is that the polymer molecules do not need to stretch to wrap around the nanoparticles which results in a more stable composite material by reducing the loss of conformational entropy of the macromolecule.[36,37]

In this paper, we extend our studies to investigate the control of the organization of the PAAm-stabilized AuNPs based on the nanocomposite solution pH. We show that the composite forms discrete, chainlike assemblies or clusters that resemble micellar structures and displays distinct optical properties that depend on the solution pH. The formation of the different assemblies occurs due to changes in polymer morphology at different pH and the role of the polymer was confirmed by ligand exchange reactions. We also present investigations of the changes in the optical properties and the stability of the nanocomposite upon reversible switching of the solution pH.

Results and Discussion

Synthesis of PAAm−AuNPs Composites and Study of pH Effects. Gold nanoparticles were synthesized according to Scheme 1 by adding 10 mL of 0.32 M PAAm to a 190 mL of boiling aqueous solution containing 0.051 mmol of tetrachloroauric acid. 30 min after addition of polymer, the colorless homogeneous solution became purple. The reduction process was monitored by UV−vis absorption spectroscopy. A slow and steady increase of the absorption maxima was observed. The process took almost 220 min to reach a stable λ_{max} of 517 nm (Figure 1A), and the final solution was a brownish-red color. The gold salt solution had a pH of 3.1 before addition of polymer, and after the reduction, the nanocomposite solution pH was 9.2. Transmission electron microscopy (TEM) analysis of the solution showed the presence of spherical nanoparticles

* Corresponding author. E-mail: shumaker-parry@chem.utah.edu.

10.1021/ma800407s CCC: $40.75 © 2008 American Chemical Society
Published on Web 05/22/2008

Scheme 1. Synthesis of Stable PAAm−AuNP Composite in Water

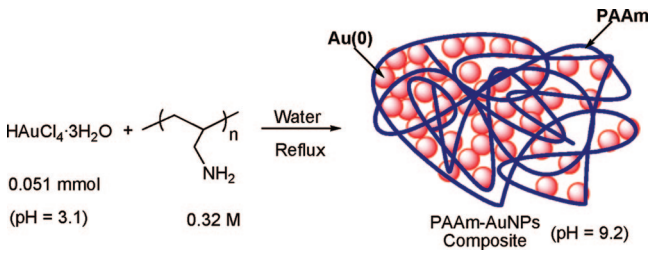

(2.6 ± 0.7 nm) organized in clusters resembling micelle-like assemblies along with individual AuNPs, as shown in Figure 1B.

We investigated the effect of pH on the PAAm−AuNPs composite by monitoring changes in the position of the SPR band as the solution pH was adjusted. First, 20 mL of the PAAm−AuNPs composite solution (pH 9.2) was transferred to a glass beaker, and 1 M HCl was added to adjust the pH to 1.5. The solution became darker in color and displayed a plasmon resonance peak at 525 nm, which is 8 nm red-shifted in comparison to the starting AuNP solution (see inset of Figure 2). In a similar fashion, the SPR band of the AuNPs was investigated for a wide range of solution pH values. The results are shown in Figure 2. As the solution was brought to a pH of 12.5 by adding 1 M NaOH, the absorption maximum (λ_{max}) was 519 nm, which is a 6 nm blue shift compared to the band position of the solution at pH 1.5. Further incremental pH adjustments did not change the position of the SPR band of the composite. The intensity of the SPR band of AuNPs was lower at pH 1.5 and 12.5 compared to the original composite solution at a pH of 9.2. This is due to a dilution effect as a result of pH

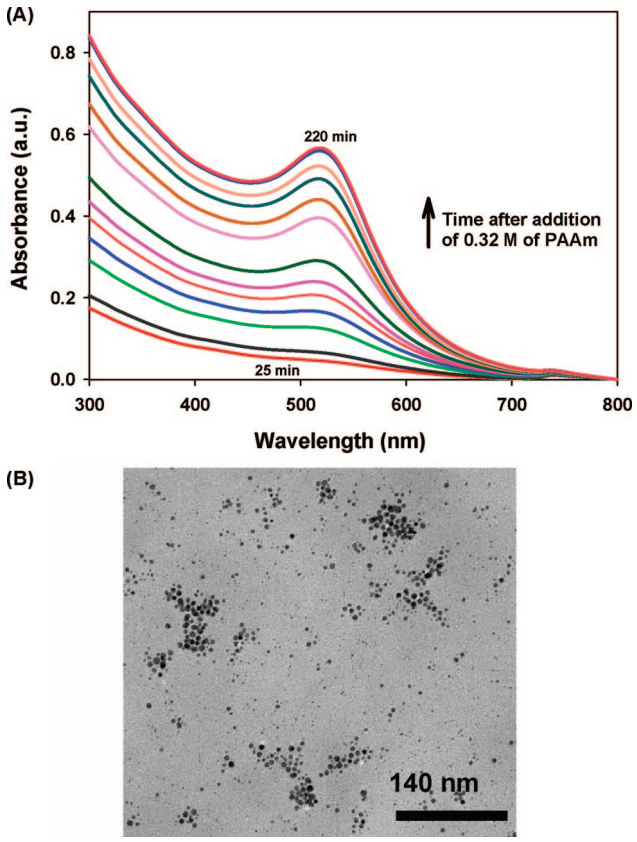

Figure 1. UV−vis absorption spectra (A) and TEM image (B) of AuNPs synthesized using 0.32 M PAAm.

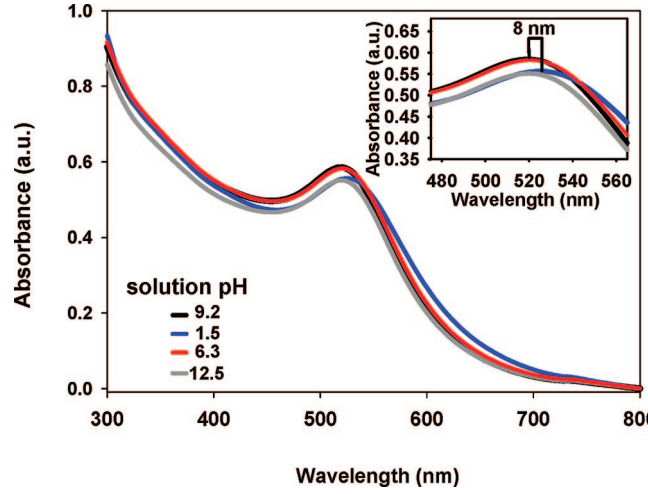

Figure 2. UV−vis absorption spectra of PAAm−AuNPs composite at different solution pH.

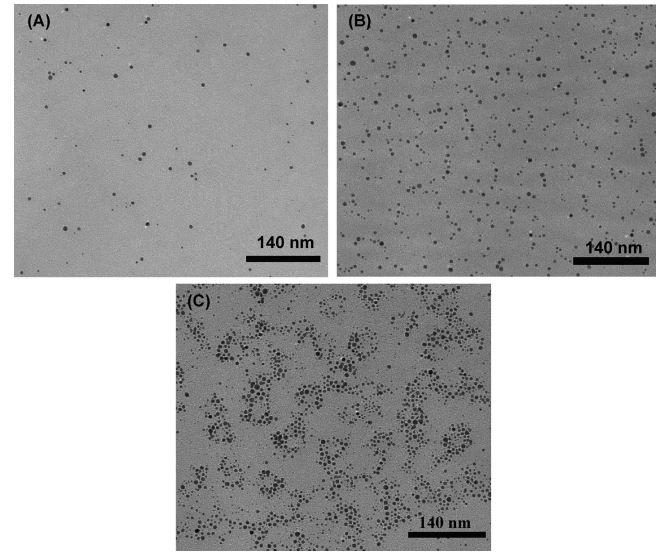

Figure 3. TEM images of PAAm stabilized AuNPs at pH of (A) 1.5, (B) 3.5, and (C) 12.5.

adjustment by adding either acid or base solution. No AuNP precipitation was observed.

The particle size and morphology of the AuNPs at different pH were investigated by TEM (see Figure 3). TEM analysis showed that the size of the AuNPs from the initial synthesis (i.e., before the pH was adjusted) was 2.6 ± 0.7 nm, and the AuNPs formed clusters. At the acidic pH of 1.5, we observed the formation of well-dispersed individual spherical particles and no cluster formation. The pH-dependent organization of the AuNPs could be explained by changes in the local environment. At pH 1.5 all of the amine groups of PAAm should be protonated, and repulsion between the positively charged polymer chains would result in the particles staying apart. Alternatively, at this acidic pH, a high concentration of charged ions could adsorb on the surfaces of the AuNPs and create an electrical double layer around the particle surface, also leading to electrostatic repulsion. No matter what the origin is, the repulsion results in the increased dispersion of the AuNPs. As the solution pH was adjusted to 3.5, the TEM analysis showed the formation of chainlike assemblies with regular interparticle spacing. From the TEM results in Figure 3B, we expect that at this pH the pendent amine groups on the polymer are protonated, and due to electrostatic repulsion, the polymer chain is fully extended. When the solution pH was adjusted to 12.5 from 9.2,

Table 1. UV−vis Absorption Maxima and Particle Sizes of AuNPs at Different pH[a]

initial solution pH	final solution pH	UV−vis abs maxima (λ_{max}, nm)	particle size (nm)[b]
9.2[c]		517	2.6 (0.7)
9.2	1.5	525	3.3 (0.8)
9.2	3.5	525	3.2 (0.7)
9.2	6.3	519	2.8 (0.7)
9.2	12.5	519	2.7 (0.7)

[a] At least 200 particles were counted to determine the particle size and standard deviation. [b] The number in parentheses represents the standard deviation. [c] pH of the final solution when 0.051 mmol of gold salt was reduced in the presence of 0.32 M of PAAm.

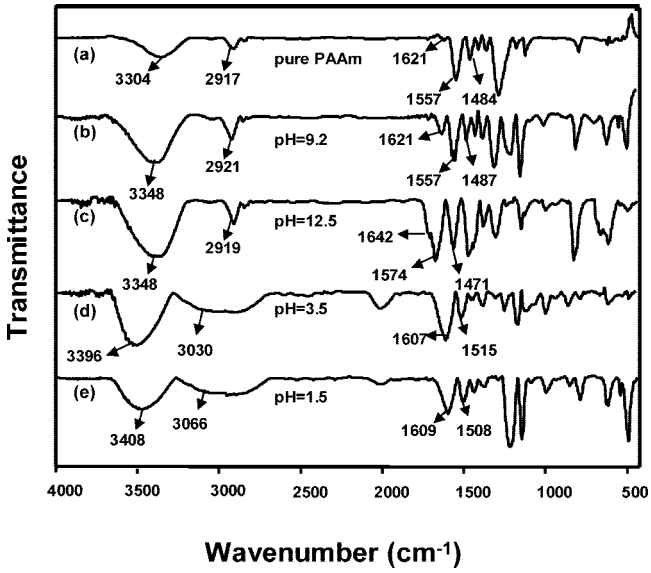

Figure 4. FTIR spectra of PAAm−AuNPs composites at solution pH of (b) 9.2, (c) 12.5, (d) 3.5, and (e) 1.5. The spectrum in (a) is for pure PAAm.

we observed the presence of clusters of AuNPs (Figure 3C). Under basic conditions, the polymer will be uncharged and should assume a more compact conformation, which would lead to a more aggregated state of AuNPs. However, because the surfaces of the AuNP are already coated with polymer molecules, dense aggregates cannot form. Results from a comparison study of UV−vis absorption maxima and particle size of the PAAm−AuNPs composites at various solution pH values are presented in Table 1.

To investigate the nature and structure of the polymer at different solution pH, the PAAm−AuNPs composite was analyzed by Fourier transform infrared (FTIR) spectroscopy. Figure 4 presents the FTIR spectra of the nanocomposite material at different solution pH values. The as-prepared PAAm−AuNPs composite solution displayed a basic pH of 9.2. At this pH the polymer should be unprotonated, which was confirmed by FTIR analysis. The spectrum was almost identical to pure PAAm, which suggests that the polymer stabilized the AuNPs by association through unprotonated amine groups from the polymer backbone. Further increase of solution pH to 12.5 did not result in a substantially different IR spectrum. The IR analysis of the PAAm−AuNPs composite also was performed at solution pH values of 3.5 and 1.5. In both low-pH cases, strong peaks at 1607 or 1609 cm^{-1} and 1517 or 1508 cm^{-1} are attributed to the asymmetric and symmetric NH_3^+ deformation, respectively.[38] The peak at 3066 cm^{-1} is assigned to the symmetric NH_3^+ stretching band.[39,40] At high acidic conditions, the amine groups are expected to be protonated, resulting in the presence of different IR signatures for the NH_3^+ group at pH 3.5 and 1.5 compared to pH of 9.2 or 12.5. The IR data

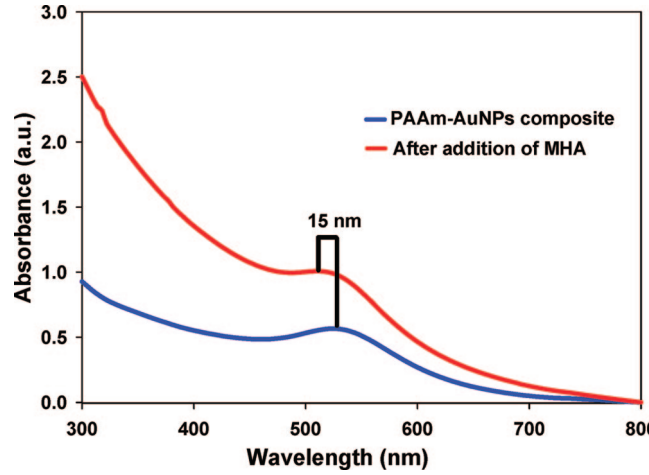

Figure 5. Comparison of UV−vis absorption maxima of PAAm−AuNP composite before and after ligand exchange reaction at pH 3.5.

confirm protonation of the PAAm amine groups in the composite material. At those low pH values, the AuNPs also were stable in solution, which suggests that protonated amine groups have the ability to stabilize the nanoparticles and keep them in a dispersed state.

Ligand Exchange Studies of PAAm−AuNPs under Different pH Conditions. So far we have shown that different assemblies of AuNPs were generated due to the structural modification of PAAm in the nanocomposite solution upon changing the solution pH. To further validate the TEM and FTIR results, ligand exchange reactions were performed. In the exchange reaction, addition of foreign ligand to a solution of ligand-protected nanoparticles results in the displacement of the protecting shell on the nanoparticle surface with the foreign ligand. Previously, different thiolated molecules have been investigated for exchange reactions, and it was observed that the exchange reactions are strongly dependent on the nature of the ligand as well as the reaction medium.[41,42] We used thiolated molecules in the ligand exchange because of the ability of these molecules to displace the amine groups from the surface of the nanoparticles to produce thiol-stabilized AuNPs due to the strong gold−sulfur interactions.[43] In addition, it has been reported that thiolated ligand containing acid groups undergoes protonation/deprotonation depending on solution pH.[44] We used 16-mercaptohexadecanoic acid (MHA) for the exchange reaction at different nanocomposite solution pH values. The ligand exchange reactions with MHA on PAAm−AuNPs composite at pH values of 1.5, 3.5, and 12.5 were investigated. We could expect that, as the thiol molecules adsorb on the AuNP surface, the assemblies which were generated due to the presence of the PAAm would be changed and different assemblies would be formed.

In the first ligand exchange experiment 1 mL of 10 mM of MHA solution was added to 10 mL of PAAm stabilized AuNPs solution at pH 1.5, and the reaction mixture was stirred for 30 min at room temperature. During the stirring time, the solution color changed to purple from a brownish-red color, and eventually particle precipitation was observed. The solid precipitate was then centrifuged out, and both the purple solid and the purple liquid parts were collected. The purple liquid showed an absorbance maximum at 522 nm in UV−vis spectroscopy analysis (see Supporting Information). The solid portion was redispersed in 10 mL of ethanol which produced a purple solution (λ_{max} of 522 nm) (see Supporting Information). The precipitation can be explained by the addition of the MHA to the PAAm−AuNPs composite at a pH of 1.5. After the thiol displaced the polymer amine groups to bind to the gold surface,

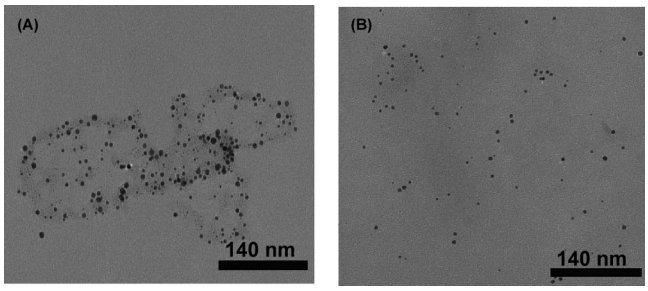

Figure 6. TEM images of the MHA-stabilized gold nanoparticles at solution pH values of (A) 1.5 and (B) 12.5.

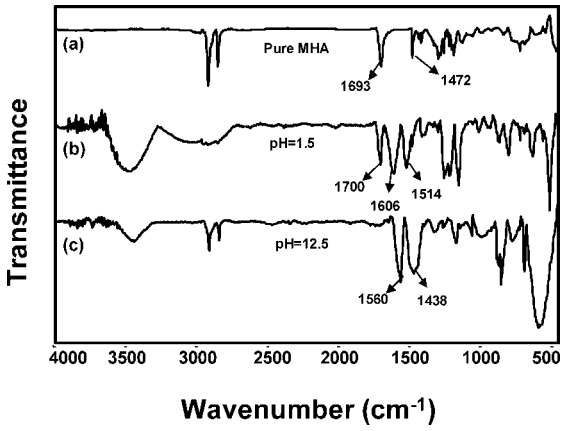

Figure 7. FTIR spectra after ligand exchange of PAAm−AuNPs conjugates with MHA at pH values of (b) 1.5 and (c) 12.5. The spectrum in (a) is for pure MHA.

a solid was formed due to hydrogen bonding between MHA terminal acid groups in the ligand shell on the AuNPs.

A similar ligand exchange reaction also was performed with PAAm−AuNPs composites after the solution pH was adjusted to 3.5. After addition of MHA to the polymer-stabilized nanoparticle solution and stirring for 5 min, the color of the solution changed to purplish-red and displayed a SPR band (λ_{max}) at 510 nm, which is 15 nm blue-shifted compared to the starting solution (λ_{max} of 525 nm) as shown in Figure 5. The SPR wavelength (λ_{max}) of AuNPs is strongly dependent on the local dielectric environment of the nanoparticles.[45–47] As MHA molecules displaced the amine groups and the polymer from the AuNPs' surfaces, the local dielectric environment changed, resulting in the 15 nm blue shift of the SPR band. In another experiment, the same MHA solution was added to the polymer−nanocomposite solution at pH 12.5. After addition of MHA and stirring for 30 min, the color of the solution changed from brownish-red to purple (λ_{max} of 521 nm) (see Supporting Information), and the AuNPs were stabilized by the MHA molecules. The color change is likely due to the new ligand environment around the particles. As no particle precipitation was observed, it is obvious that the MHA stabilized the AuNPs.

All of the ligand exchange samples at different solution pH were analyzed by TEM. In the case of pH 1.5, the TEM showed formation of aggregated AuNPs with an average particle size of 3.4 ± 0.8 nm (see Figure 6A). On the other end of the spectrum at pH 12.5, well-dispersed, individual AuNPs were observed with no evidence of clusters (see Figure 6B). This result also validates our hypothesis that the AuNP clusters were formed because of the presence of polymer in the solution. When the polymer molecules were displaced from the nanoparticles' surfaces through the ligand exchange reaction with MHA, only well-dispersed individual nanoparticles were observed. Under basic conditions at pH 12.5, all of the carboxylic acid (−COOH) groups should be converted to carboxylate groups ($-COO^-$). Because of electrostatic repulsion between the carboxylate groups, the particles were well dispersed as shown in the TEM images. When MHA is added to the PAAm−AuNPs composite at a pH of 1.5, the thiol group binds to the gold surface, and a solid was formed due to hydrogen bonding between MHA acid groups.

The post ligand exchange samples were analyzed by FTIR spectroscopy to confirm the nature of carboxylic acid groups in the MHA. Figure 7a presents the spectrum of pure MHA and the characteristic peak of the CO stretching band of carboxylic acid at 1693 cm^{-1}.[48] The ligand exchange sample at pH 1.5 displayed the peak at 1700 cm^{-1}, which is a 7 cm^{-1} peak shift to a higher wavenumber compared to the pure MHA sample and could be due to hydrogen bonding between −COOH groups. This hydrogen bonding also correlates with the observed particle aggregation in the TEM analysis described above. The spectrum in Figure 7c shows a peak at 1560 cm^{-1} corresponding to the carboxylate ($-COO^-$) signature,[49–51] which is very significant, as in the alkaline medium most of the acid will be deprotonated. Previously, it has been reported that at alkaline pH conditions, when gold nanoparticles were functionalized with alkanethiol containing COO^- terminal groups, the particles remained in their dispersive state due to charge repulsion,[52,53] which is what was observed in the TEM analysis (see Supporting Information). The IR data also show peaks at 1606 and 1514 cm^{-1} which are due to different NH_3^+ stretching bands originating from the PAAm. The ligand exchange reactions provided confirmation of the key role of PAAm in the assemblies formed by the AuNPs at different pH which likely induced structural modification of the PAAm molecules.

Reversibility Study of PAAm−AuNPs Composite Response to Solution pH Changes. For applications in optical based sensors, it is important to investigate the stability of the polymer−nanoparticle composite material as well as the pH-

Scheme 2. Reversible Changes in pH-Dependent Nanocomposite Organization

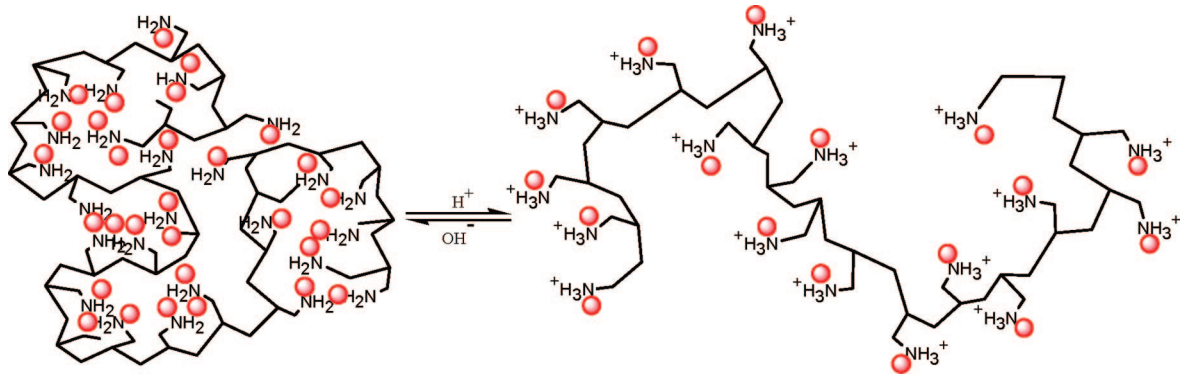

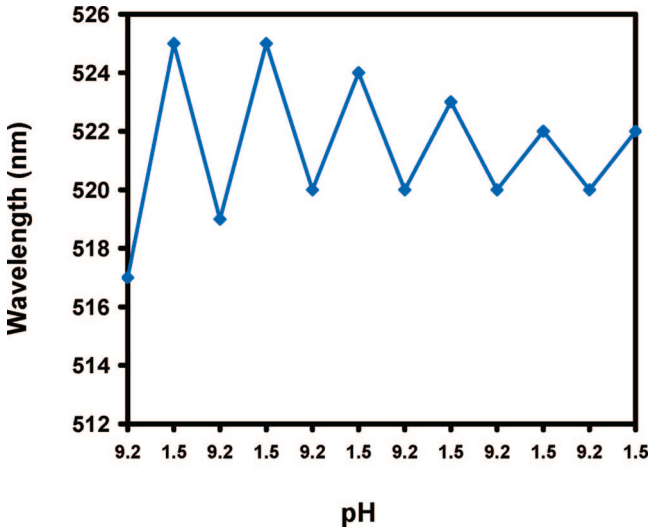

Figure 8. Optical response of PAAm−AuNPs composite as the solution pH was cycled.

dependent optical response of the AuNPs incorporated in the polymer matrix. We already have demonstrated that both the spatial arrangement and the optical response of the PAAm−AuNPs composite are sensitive to the nanocomposite solution pH. We also investigated the stability of the composite materials in response to repeated changes of the solution pH as depicted in Scheme 2.

Previously, we observed that the AuNPs in the polymer matrix display distinct absorption maxima (λ_{max}) in the UV−vis spectra. We adapted the same approach to monitor the optical response of the nanoparticles in the composite with cycling of the solution pH. The position of the SPR band for the nanocomposite solution was measured while the pH of the sample was repeatedly cycled between 1.5 and 9.2 by addition of HCl and NaOH solutions. The results are presented in Figure 8. At pH 9.2 the λ_{max} of the composite solution was 517 nm, and at pH 1.5, the maximum shifted to 525 nm. During the cycling process, a gradual blue shift of the λ_{max} at pH 1.5 was observed, which could be due to dilution effects of the solution or accumulation of NaCl, which changes the ionic strength of the solution.[54] After five cycles, a stable λ_{max} of 522 nm at both pH 9.2 and 1.5 was observed.

After five cycles at pH 1.5, the sample was analyzed by TEM to determine the organization of the AuNPs. TEM analysis showed that the particles were well dispersed with an average diameter of 3.4 ± 1.1 nm (see Supporting Information), and no large aggregates were observed. As shown in Table 1, the size of the AuNPs was 3.3 ± 0.8 nm at a pH of 1.5. The particle size at pH 1.5 after five repeated pH change cycles was 3.4 ± 1.1 nm. The nanoparticle morphology was nearly unchanged. The data clearly suggest that the ability of the polymer to protect the AuNPs from agglomeration after five cycles of pH changes is quite remarkable, and the original composition of the PAAm−AuNP material is maintained.

Conclusions

In conclusion, we have shown that poly(allylamine)-stabilized gold nanoparticles produced different assemblies as the pH of the nanocomposite solution changed. The formation of these assemblies occurred due to the pH-induced structural changes of the polymers as evident from FTIR spectra. The role of the polymer in the pH-sensitive organization of the AuNPs in the composite was further validated using ligand exchange reactions by addition of thiolated ligand to the nanocomposite solution. The PAAm−AuNPs were able to undergo at least five reversible assembly/dispersion cycles which were observed by monitoring optical changes of the composite. We are investigating the application of the PAAm−AuNPs composites for SPR sensing.

Experimental Section

Materials. $HAuCl_4 \cdot 3H_2O$, poly(allylamine) (PAAm, 20 wt % solution in water, M_w ca. 65 000), and 16-mercaptohexadecanoic acid (MHA) were purchased from Aldrich and used as received. Water used during the synthetic procedures was purified using a NANOpure Diamond (Barnstead, Nanopure water 17.8 MΩ·cm). All glassware was washed with Aqua-regia (HCl:HNO_3 = 3:1) and rinsed with a copious amount of Nanopure water. The solution pH was adjusted using either 1.0 M HCl or 0.2 M NaOH solution.

pH Measurements, Spectroscopy, and Microscopy. pH measurements were carried out using an InLab 413 probe at room temperature with an accuracy of ±0.2 pH units. Before each measurement, the probe was calibrated with fresh 7.0 and 4.0 standard Merck buffer solutions. Absorption spectra (250−800 nm) were collected using a Perkin-Elmer Lambda 19 UV/vis/NIR spectrophotometer. The samples of PAAm−AuNPs were taken from the reaction vessel and analyzed without a cooling step. A Perkin-Elmer Spectrum 100 FT-IR spectrometer was used for IR analysis. Transmission electron microscopy (TEM) micrographs were obtained using a Tecnai-12 instrument operating at 100 kV accelerating voltage. For TEM analysis, one drop of solution was deposited on a 150 mesh Formvar-coated copper grid, and excess solution was removed by wicking with a filter paper to avoid particle aggregation. The particle size analysis was conducted by analyzing 200 particles in the TEM images using Scion Image Beta 4.02 Software. In Scion Image, after setting the known distance and unit, the "Analyze Particle" parameter was used to generate a table of particle diameters. This table was then exported into Microsoft Excel 2007 where statistical analysis was performed and a histogram was plotted.

Synthesis of PAAm−AuNPs Composite. 0.051 mmol of $HAuCl_4 \cdot 3H_2O$ (20 mg) was dissolved in 190 mL of Nanopore water in a three-neck round-bottom flask, which displayed a stable pH of 3.1. After the solution was allowed to reflux with constant stirring, 10 mL of 0.32 M PAAm aqueous solution was added to the gold salt solution. The reaction was monitored by UV−vis spectroscopy and allowed to proceed until the amplitude of the absorption spectrum reached a maximum. The color of the final product solution was brownish-red. Once the reaction was complete, the solution was allowed to cool to room temperature and then stored in a cleaned brown-glass container for further experiments. The pH of the solution was 9.2.

pH-Dependent Investigations of AuNP Assemblies. A 20 mL aliquot of PAAm−AuNP composite was transferred to a glass container and adjusted to the appropriate pH by adding either 1 M HCl or 1 M NaOH solution with constant stirring until the pH was stable. The solution was then stirred for another 10 min before analyzing by UV/vis/NIR spectroscopy. One drop of the same solution was deposited on a TEM grid for morphological analysis.

Ligand Exchange Reactions. 10 mL of as-synthesized PAAm−AuNP solution (pH = 9.2) was transferred to a 100 mL beaker. The solution pH was then adjusted to 12.5 by adding 1 M NaOH solution with constant stirring. At this point, 1 mL of 10 mM 16-mercaptohexadecanoic acid (MHA) solution was added, and stirring was continued for another 30 min. After 30 min of stirring the color of the solution turned from brownish-red to purple. The purple solution was then analyzed by UV−vis absorption spectroscopy, TEM, and FTIR. A similar methodology was followed to study the ligand exchange reaction at pH 1.5. In this case, the pH of the nanocomposite solution was adjusted using 1 M HCl solution.

Supporting Information Available: Additional UV−vis absorption spectra, TEM images for ligand exchange study, and particle size analysis table before and after ligand exchange reactions. This material is available free of charge via Internet at http://pubs.acs.org.

References and Notes

(1) Storhoff, J. J.; Elghanian, R.; Mucic, R. C.; Mirkin, C. A.; Letsinger, R. L. *J. Am. Chem. Soc.* **1998**, *120*, 1959–1964.
(2) He, L.; Musick, M. D.; Nicewarner, S. R.; Salinas, F. G.; Benkovic, S. J.; Natan, M. J.; Keating, C. D. *J. Am. Chem. Soc.* **2000**, *122*, 9071–9077.
(3) Katz, E.; Willner, I. *Angew. Chem., Int. Ed.* **2004**, *43*, 6042–6108.
(4) Pissuwan, D.; Valenzuela, S. M.; Cortie, M. B. *Trends Biotechnol.* **2006**, *24*, 62–67.
(5) Lim, J. K.; Joo, S.-W. *Appl. Spectrosc.* **2006**, *60*, 847–852.
(6) Majid, E.; Hrapovic, S.; Liu, Y.; Male, K. B.; Luong, J. H. T. *Anal. Chem.* **2006**, *78*, 762–769.
(7) Stuart, D. A.; Yonzon, C. R.; Zhang, X.; Lyandres, O.; Shah, N. C.; Glucksberg, M. R.; Walsh, J. T.; Van Duyne, R. P. *Anal. Chem.* **2005**, *77*, 4013–4019.
(8) Maier, S. A.; Kik, P. G.; Atwater, H. A. *Appl. Phys. Lett.* **2002**, *81*, 1714–1716.
(9) Maier, S. A.; Kik, P. G.; Atwater, H. A.; Meltzer, S.; Harel, E.; Koel, B. E.; Requicha, A. A. G. *Nat. Mater.* **2003**, *2*, 229–232.
(10) Salerno, M.; Krenn, J. R.; Hohenau, A.; Ditlbacher, H.; Schider, G.; Leitner, A.; Aussenegg, F. R. *Opt. Commun.* **2005**, *248*, 543–549.
(11) Chauhan, B. P. S.; Sardar, R. *Macromolecules* **2004**, *37*, 5136–5139.
(12) Corbierre, M. K.; Cameron, N. S.; Sutton, M.; Mochrie, S. G. J.; Lurio, L. B.; Ruhm, A.; Lennox, R. B. *J. Am. Chem. Soc.* **2001**, *123*, 10411–10412.
(13) Hussain, I.; Graham, S.; Wang, Z.; Tan, B.; Sherrington, D. C.; Rannard, S. P.; Cooper, A. I.; Brust, M. *J. Am. Chem. Soc.* **2005**, *127*, 16398–16399.
(14) Kim, B. J.; Bang, J.; Hawker, C. J.; Kramer, E. J. *Macromolecules* **2006**, *39*, 4108–4114.
(15) Lee, H.; Choi, S. H.; Park, T. G. *Macromolecules* **2006**, *39*, 23–25.
(16) Li, B.; Li, C. Y. *J. Am. Chem. Soc.* **2007**, *129*, 12–13.
(17) Lowe, A. B.; Sumerlin, B. S.; Donovan, M. S.; McCormick, C. L. *J. Am. Chem. Soc.* **2002**, *124*, 11562–11563.
(18) Wuelfing, W. P.; Gross, S. M.; Miles, D. T.; Murray, R. W. *J. Am. Chem. Soc.* **1998**, *120*, 12696–12697.
(19) Wyrwa, D.; Beyer, N.; Schmid, G. *Nano Lett.* **2002**, *2*, 419–421.
(20) Barnes, K. A.; Karim, A.; Douglas, J. F.; Nakatani, A. I.; Gruell, H.; Amis, E. J. *Macromolecules* **2000**, *33*, 4177–4185.
(21) Yurekli, K.; Karim, A.; Amis, E. J.; Krishnamoorti, R. *Macromolecules* **2003**, *36*, 7256–7267.
(22) Cheng, J. Y.; Rose, C. A.; Chan, V. Z. H.; Thomas, E. L.; Lammertink, R. G. H.; Vancso, G. J. *Adv. Mater.* **2001**, *13*, 1174–1178.
(23) Hong, Y.; Sen, A. *Chem. Mater.* **2007**, *19*, 961–963.
(24) Kumar, S. S.; Kumar, C. S.; Mathiyarasu, J.; Phani, K. L. *Langmuir* **2007**, *23*, 3401–3408.
(25) Negishi, Y.; Takasugi, Y.; Sato, S.; Yao, H.; Kimura, K.; Tsukuda, T. *J. Am. Chem. Soc.* **2004**, *126*, 6518–6519.
(26) Song, H.; Rioux, R. M.; Hoefelmeyer, J. D.; Komor, R.; Niesz, K.; Grass, M.; Yang, P.; Somorjai, G. A. *J. Am. Chem. Soc.* **2006**, *128*, 3027–3037.
(27) Tokareva, I.; Minko, S.; Fendler, J. H.; Hutter, E. *J. Am. Chem. Soc.* **2004**, *126*, 15950–15951.
(28) Hooper, J. B.; Schweizer, K. S. *Macromolecules* **2006**, *39*, 5133–5142.
(29) Starr, F. W.; Schroder, T. B.; Glotzer, S. C. *Macromolecules* **2002**, *35*, 4481–4492.
(30) Mackay, M. E.; Tuteja, A.; Duxbury, P. M.; Hawker, C. J.; Van Horn, B.; Guan, Z.; Chen, G.; Krishnan, R. S. *Science* **2006**, *311*, 1740–1743.
(31) Tyagi, S.; Lee, J. Y.; Buxton, G. A.; Balazs, A. C. *Macromolecules* **2004**, *37*, 9160–9168.
(32) Guo, Y.; Ma, Y.; Xu, L.; Li, J.; Yang, W. *J. Phys. Chem. C* **2007**, *111*, 9172–9176.
(33) Li, D.; He, Q.; Cui, Y.; Li, J. *Chem. Mater.* **2007**, *19*, 412–417.
(34) Shimada, T.; Ookubo, K.; Komuro, N.; Shimizu, T.; Uehara, N. *Langmuir* **2007**, *23*, 11225–11232.
(35) Sardar, R.; Park, J. W.; Shumaker-Parry, J. S. *Langmuir* **2007**, *23*, 11883–11889.
(36) Balazs, A. C.; Emrick, T.; Russell, T. P. *Science* **2006**, *314*, 1107–1110.
(37) Thompson, R. B.; Ginzburg, V. V.; Matsen, M. W.; Balazs, A. C. *Science* **2001**, *292*, 2469–2472.
(38) Kumar, A.; Mandal, S.; Selvakannan, P. R.; Pasricha, R.; Mandale, A. B.; Sastry, M. *Langmuir* **2003**, *19*, 6277–6282.
(39) Bonazzola, C.; Calvo, E. J.; Nart, F. C. *Langmuir* **2003**, *19*, 5279–5286.
(40) Itano, K.; Choi, J.; Rubner, M. F. *Macromolecules* **2005**, *38*, 3450–3460.
(41) Hostetler, M. J.; Green, S. J.; Stokes, J. J.; Murray, R. W. *J. Am. Chem. Soc.* **1996**, *118*, 4212–4213.
(42) Templeton, A. C.; Wuelfing, W. P.; Murray, R. W. *Acc. Chem. Res.* **2000**, *33*, 27–36.
(43) Li, B.; Ni, C.; Li, C. Y. *Macromolecules* **2008**, *41*, 149–155.
(44) Basu, S.; Ghosh, S. K.; Kundu, S.; Panigrahi, S.; Praharaj, S.; Pande, S.; Jana, S.; Pal, T. *J. Colloid Interface Sci.* **2007**, *313*, 724–734.
(45) Haes, A. J.; Zou, S.; Schatz, G. C.; VanDuyne, R. P. *J. Phys. Chem. B* **2004**, *108*, 109–116.
(46) Haynes, C. L.; Van Duyne, R. P. *J. Phys. Chem. B* **2001**, *105*, 5599–5611.
(47) Jensen, T. R.; Malinsky, M. D.; Haynes, C. L.; Van Duyne, R. P. *J. Phys. Chem. B* **2000**, *104*, 10549–10556.
(48) Zheng, W.; Maye, M. M.; Leibowitz, F. L.; Zhong, C. J. *Anal. Chem.* **2000**, *72*, 2190–2199.
(49) Kepley, L. J.; Crooks, R. M.; Ricco, A. J. *Anal. Chem.* **1992**, *64*, 3191–3193.
(50) Nuzzo, R. G.; Dubois, L. H.; Allara, D. L. *J. Am. Chem. Soc.* **1990**, *112*, 558–569.
(51) Smith, E. L.; Porter, M. D. *J. Phys. Chem.* **1993**, *97*, 8032–8038.
(52) Simard, J.; Briggs, C.; Boal, A. K.; Rotello, V. M. *Chem. Commun.* **2000**, 1943–1944.
(53) Su, C.-H.; Wu, P.-L.; Yeh, C.-S. *Bull. Chem. Soc. Jpn.* **2004**, *77*, 189–193.
(54) Jung, Y. H.; Lee, K.-B.; Kim, Y.-G.; Choi, I. S. *Angew. Chem., Int. Ed.* **2006**, *45*, 5960–5963.

MA800407S